Citation: Blood Cancer Journal (2011) 1, e15; doi:10.1038/bcj.2011.11

www.nature.com/bcj

ORIGINAL ARTICLE

The identification of irreversible rituximab-resistant lymphoma caused by *CD20* gene mutations

Y Mishima[1,2], Y Terui[1], K Takeuchi[3], Y Matsumoto-Mishima[1], S Matsusaka[1], R Utsubo-Kuniyoshi[1,2] and K Hatake[1]

[1]*Department of Clinical Chemotherapy, Cancer Chemotherapy Center, Japanese Foundation for Cancer Research, Tokyo, Japan;* [2]*Olympas Bio-Imaging Lab, Cancer Chemotherapy Center, Japanese Foundation for Cancer Research, Tokyo, Japan and* [3]*Division of Pathology, Cancer Institute, Japanese Foundation for Cancer Research, Tokyo, Japan*

C-terminal mutations of CD20 constitute part of the mechanisms that resist rituximab therapy. Most CD20 having a C-terminal mutation was not recognized by L26 antibody. As the exact epitope of L26 has not been determined, expression and localization of mutated CD20 have not been completely elucidated. In this study, we revealed that the binding site of L26 monoclonal antibody is located in the C-terminal cytoplasmic region of CD20 molecule, which was often lost in mutated CD20 molecules. This indicates that it is difficult to distinguish the mutation of CD20 from under expression of the CD20 protein. To detect comprehensive CD20 molecules including the resistant mutants, we developed a novel monoclonal antibody that recognizes the N-terminal cytoplasm region of CD20 molecule. We screened L26-negative cases with our antibody and found several mutations. A rituximab-binding analysis using the cryopreserved specimen that mutation was identified in CD20 molecules indicated that the C-terminal region of CD20 undertakes a critical role in presentation of the large loop in which the rituximab-binding site locates. Thus, combination of antibodies of two kinds of epitope permits the identification of C-terminal CD20 mutations associated with irreversible resistance to rituximab and may help the decision of the treatment strategy.
Blood Cancer Journal (2011) **1,** e15; doi:10.1038/bcj.2011.11; published online 8 April 2011
Keywords: B-cell lymphomas; mutations; antibody therapy; CD20; rituximab

Introduction

Previously, we reported that gene mutations of *CD20* were somehow involved in resistance to rituximab therapy, and we proposed that C-terminal deletion mutations of CD20 might be related to relapse/resistance after rituximab therapy.[1] Many of these C-terminal truncated CD20 molecules were not recognized by the L26 monoclonal antibody used routinely in most clinical laboratories. Therefore, expression of CD20 seemed to have been completely lost for these lymphomas. However, an immunohistochemical study using a polyclonal antibody showed that some kind of C-terminal truncated CD20 was present in cytoplasm, so it was possible that the epitope of L26 was lost by gene mutations.[1] L26 recognizes the cytoplasmic region of CD20 molecules, but no more detailed information about its epitope had been reported.[2,3] In this study, we determine a recognition site of L26 by using a series of deletion mutants of CD20 molecules. In addition, to detect every one of the mutated CD20 molecules, we developed new antibodies that recognize the N-terminal region of CD20 molecules. We used these antibodies to identify cells that have CD20 molecules with abnormalities in the C-terminal cytoplasmic region. We characterized these mutated CD20 molecules using living primary lymphoma cells.

Correspondence: Dr K Hatake, Department of Clinical Oncology and Hematology, Cancer Institute Hospital, Japanese Foundation for Cancer Research, 3-8-31, Ariake Koto-ku, Tokyo 135-8550, Japan.
E-mail: khatake@jfcr.or.jp
Received 28 October 2010; revised 7 January 2011; accepted 1 February 2011

Materials and methods

Cells, viruses and DNA constructs

The coding region of the *CD20* gene was amplified by reverse transcription PCR (RT-PCR) from RNA extracted from a Burkitt's lymphoma cell line, Raji, and was cloned into a pDON-AI retroviral vector (Takara, Ohtsu, Japan). A series of deletion mutants of CD20 in the C-terminal cytoplasmic region was constructed by inserting stop codons after nucleotides encoding E281, E263, E245, V228 and G210. Retroviruses carrying wild type and deletion mutants of *CD20*, together with mock construct, were produced with the transient retrovirus packaging cell line G3T-hi (Takara) according to the manufacturer's protocol. Packaged retrovirus vectors were then used to infect a myeloma cell line, KMS12PE,[4] with subsequent selection using 500 μg/ml G418.

For the transfection of mutant *CD20* gene, whole coding region of *CD20* complementary DNA (cDNA) prepared by RT-PCR of total RNA isolated from the patient cells was cloned into first cassette of a bicistronic retrovirus vector carrying a green fluorescent protein (Takara). Bicistronic expression of ZsGreen is facilitated by internal ribosomal entry site only when *CD20* mutant gene was translated, enabling the efficient selection of transformed cells.

Generation of monoclonal antibody secreting hybridomas

A synthetic peptide corresponding to residues 23–36 of human CD20 with one additional cysteine at the N-terminus (CMQSGPKPLFRRMSS) was synthesized. The peptide was coupled with keyhole limpet hemocyanin. BALB/c mice were primed with a subcutaneous injection of the keyhole limpet hemocyanin-conjugated synthetic peptide emulsified in Freund's complete adjuvant. Mice were boosted four times at two-week intervals with the same antigen. Mice that developed antibodies as measured by enzyme-linked immunosorbent assay with the immunizing peptide were boosted intravenously with the same peptide 4 days before splenocytes were harvested and fused to mouse myeloma cells. Hybridization and cloning were performed according to standard procedures.[5]

CD20 gene sequencing

Pleural effusion mononuclear cells were obtained by density gradient centrifugation using Ficoll-Hypaque 1.077 (Sigma,

St Louis, MO, USA). The isolated mononuclear cells then underwent negative immunomagnetic selection using a B Cell Isolation Kit II (Miltenyi Biotec, Bergisch Gladbach, Germany) for purifying B-linage cells. Total RNA was prepared using TRIzol reagent according to the instructions of the manufacturer (Invitrogen, Carlsbad, CA, USA) and 1 μg was subjected to reverse transcription under MMLV reverse transcriptase (Takara). To prepare cDNA-containing whole coding region of *CD20*, PCR amplification was performed from 2 μl of cDNA using primers outside of the start and the stop codon: hCD20-5′-FW (5′-GCAGCTAGCATCCAAATCAG-3′) and hCD20-3′-RV (5′-TGGTGCGTATGTGCAGAGTA-3′). To determine the sequence of the *CD20*, we performed cycle sequencing on a 3130 DNA analyzer (Applied Biosystems, Foster City, CA, USA), directly from PCR-purified products, in both directions using a BigDye Terminator Cycle Sequencing Kit v3.1 (Applied Biosystems).

Immunocytochemistry

Cells were stained by rituximab and L26 antibody (DAKO, Carpentaria, CA, USA) sequentially. Briefly, the cells were labeled by incubating in 10 μg/ml of rituximab conjugated with Alexa Fluor 647 (Invitrogen) according to previously described procedure[6] and washed twice with phosphate-buffered saline. Rituximab-labeled cells were swelled by treatment with 75 mM KCl and then were made to adhere onto collagen I-coated cover glass by brief centrifugation. After fixing and permeabilization, the specimens were exposed to L26 antibody. Subsequently, the specimens were washed and were incubated in Alexa488-conjugated goat anti-mouse IgG. Nuclear staining was performed using 5 μg/ml of 4′-6-diamidino-2-phenylindole. The preparations were screened for fluorescence with a confocal microscope (FV1000, OLYMPUS, Tokyo, Japan) using excitation wavelengths of 405, 488 and 633 nm to detect emission by nuclear staining (4′-6-diamidino-2-phenylindole), rituximab or L26 staining, respectively.

Immunohistochemistry

The tissues had been routinely fixed in 10% neutral formalin and embedded in paraffin. L26 antibody and monoclonal antibodies raised against the N-terminal cytoplasmic region of CD20 were used. The sections were deparaffinized and rehydrated in graded alcohol. For heat-induced epitope retrieval, the sections were subjected to Target Retrieval Solution, pH 9 (DAKO) at 97 °C for 40 min. The sections then were brought to an automated stainer (DAKO) by following the vendor's protocol. EnVision Plus (DAKO) and peroxidase detection methods were used.

Rituximab-binding analysis

Rituximab-binding analysis was performed according to our previously developed imaging-based procedure, with some modifications.[6] Briefly, approximately ten thousands cells of purified living lymphoma cells using a Dead cell removal kit (Miltenyi Biotec) were incubated with 10 μg/ml of anti-CD19 mAb labeled with Alexa Fluor 488 (Invitrogen) and rituximab labeled with Alexa Fluor 647 (Invitrogen) for 30 min at 4 °C. The cells were washed with phosphate-buffered saline two times and were then suspended in 4 μl of RPMI1640 medium supplemented with 10% fetal bovine serum and 5 μg/ml of Hoechist 33 342. The cell suspension was pipetted into a well made of silicon, 2.5 mm in diameter and 2 mm in depth, on a piece of cover glass. Images were collected by means of an OLYMPUS PlanApo ×60 oil objective in an OLYMPUS FV-1000 confocal microscope (OLYMPUS). The fluorophore was excited by laser at 405, 488 or 633 nm. The cells were optically sectioned along the *z*-axis, and the images were collected at 640 × 640 pixel resolution in a sequential mode to minimize the crossover between channels. The step size in the *z*-axis was 0.5 μm. For three-dimensional reconstruction, two-dimensional confocal stacks were saved in an Olympus.oib format and three-dimensional images were generated using Fluoview software (OLYMPUS).

Cell sorting and genetic analysis

The cryopreserved B-linage cells of the pleural effusion at relapse were further sorted into two fractions of the cells with high affinity to rituximab (R-high) and those of low (R-low) by using flow cytometry (FACSvantage, Becton Dickinson, Franklin Lakes, NJ, USA). The cells were labeled with rituximab conjugated with AlexaFluor488 (Invitrogen) and anti-CD19-PE (Becton Dickinson), then resuspended in phosphate-buffered saline containing 2 μg/ml of 7-AAD (Sigma) to exclude dead cells. The sorting gate used for 'R-high' was rituximab^{high}/CD19^{+}/7-AAD^{-}, and for 'R-low' was rituximab$^{low/}$CD19^{+}/7-AAD^{-}. The sorted cells were immediately used for extraction of both genomic DNA and total RNA using QIAamp DNA micro kit and RNeasy micro kit, respectively, (QIAGEN, Hilden, Germany). For amplifying the DNA-containing exon 8 of *CD20* from genomic DNA, PCR was carried out using the forward primer (5′-TTCTGTTTTZGAACATAGTTCTCCCTGTCCA-3′) and the reverse primer (5′-CAGAAAACAGAAATCACTTAAGGAGAG-3′). RT-PCR to amplify the *CD20* cDNA were performed according to the method described above. The PCR and RT-PCR products were used to determine the *CD20* gene sequence by direct sequencing method. In addition, 1 μl of RT-PCR products were cloned into a TA-cloning vector (pCR2.1, Invitrogen) and *CD20* DNA sequences of 16 clones of each RT-PCR product were determined for estimating the ratio of different sequences.

Results

To confirm the epitope of L26, we made a series of constructs of the CD20 molecules with deletion mutations in the C-terminal cytoplasmic domain and introduced them into retrovirus vectors (Figure 1a). KMS12PE cells, in which expression of CD20 is not detected immunohistologically, were then transformed, and we established six kinds of sub-lines with the various C-terminal deletion mutations of CD20. A semi-quantitative RT-PCR analysis using a primer set designed to amplify the *CD20* N-terminal region indicated that no major difference was found in *CD20* messenger RNA (mRNA) expression of the six cell lines (Figure 1b). We carried out immunocytochemical analysis using L26 and fluorescence-labeled rituximab against these six *CD20*-expressing transfectants, along with a mock transfectant and Raji cells as negative and positive controls, respectively. The cells stained by L26 antibody were only those expressing wild type (amino acid 1–297) and DM1 mutant (amino acid 1–281). On the other hand, rituximab could bind to shorter CD20 molecules, such as DM2, DM3 or DM4, as well as to the CD20 molecules recognized by L26 (Figure 1c). These results indicate that L26 antibody recognizes the C-terminal cytoplasm region of CD20 molecules and that its epitope is present in the amino-acid sequence of 264–281. The data suggest that immunohistochemistry using L26 antibody will exhibit a false negative if a deletion or a frame shift occurs upstream of this epitope. In addition, the shortest deletion mutant DM5 that lacked the C-terminal cytoplasmic region was detected by

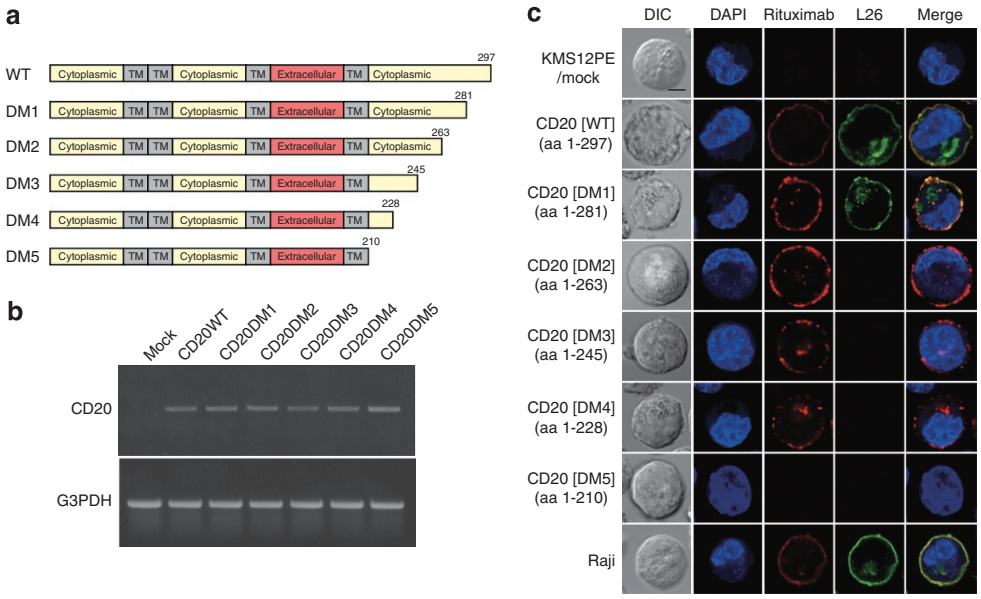

Figure 1 Search for epitopic site of L26 antibody and analysis of the extracellular exposure of CD20 molecules having C-terminal deletion mutation. (**a**) To explore the binding site of the L26 antibody, we constructed various lengths of the CD20 deletion mutant at their C-terminal cytoplasmic domains. TM: transmembrane domain. (**b**) KMS12PE cells retrovirally transduced with C-terminal truncated CD20 showed approximately similar levels of mRNA expression. (**c**) Immunocytochemical studies suggested that L26 recognizes amino-acid sequence between 264 and 281. An objective lens of $\times 60$ was used with a $\times 10$ digital zoom, bar: 5 μm. DAPI, 4′-6-diamidino-2-phenylindole; DIC, differential interference contrast; G3PDH, glyceraldehyde-3-phosphate dehydrogenase; WT, wild type.

neither L26 antibody nor rituximab. Possible reasons might include the low membrane localization of DM5 mutant and/or low stability of the post-translational product. To clarify this, we carried out western blot analysis using total cell lysate of the series of deletion mutants that were tagged by FLAG peptide at the N-terminal region of CD20 constructs. We found that the cellular protein level of the DM5 deletion mutant of CD20 was remarkably lower than that of others, suggesting that low post-translational stability may be the reason for the low antigenicity of DM5 mutant (data not shown).

To detect CD20 in the clinical specimens that acquired rituximab resistance mutations, we developed novel anti-CD20 antibodies and screened them in paraffin sections. We isolated an antibody specific for the CD20 N-terminus and named it CD20N. Using this antibody, we carried out immunohistochemistry conducted on the CD20-negative cases by L26 antibody-based analysis and found several cases with mutations in the C-terminal cytoplasm region. Among them, a cell specimen, a part of which had been cryopreserved as living cells, was included. This was pleural effusion from a patient with relapsed diffuse large cell B-cell lymphoma after complete remission following rituximab containing chemotherapy (rituximab, cyclophosphamide, adriamycin, vincristine and prednisone). This patient did not respond to further treatment with salvage therapies containing rituximab. The results of immunochemical analysis of the fibrin clot of the pleural effusion at relapse, as well as the biopsy of lymph nodes at the first examination, are shown in Figure 2. The lymph node biopsy before rituximab treatment was stained in the same way by both L26 and CD20N antibodies. However, L26 antibody did not stain at the population having mutated CD20 in the pleural effusion. On the other hand, the CD20N antibody stained almost all of the B-cell population. It should be noted that most of the cells were stained at the region of plasma membrane by CD20N antibody.

As a result of DNA sequencing of purified B cells, we found one nucleotide deletion mutation, which caused a frame shift after the amino-acid residue 251, in half of the DNA (Figure 3a). We conducted a binding analysis of rituximab using the viable cells of B-lineage purified from cryopreserved mononuclear cells. Most of these cells were CD19 positive. However, these cells consisted of two kinds of cell populations that were quite different in their affinity for rituximab (Figure 3b). Furthermore, flow cytometry analysis revealed that the fluorescent intensity of fluoro-labeled monoclonal antibody of CD20 decreased to less than one-tenth in about half of the B-cell population (Figure 3c). These results indicate that the C-terminal mutation of the *CD20* gene in this case caused abnormality of extracellular-antigen presentation, even though the protein expression and the cell membrane localization seemed to be normal.

To reveal the genetic mechanisms of the reduced antigenicity to rituximab, we conducted gene-sequencing analysis about both population of cells that differ in affinity to rituximab. The cryopreserved B lymphocytes of the pleural effusion at relapse were sorted into two fractions of cells of high affinity to rituximab (R-high) and those of low (R-low) by using flow cytometry (Figure 4a). Then genomic DNA and total RNA from each fraction were extracted. The results of DNA sequencing of exon 8 of *CD20* in which the mutation was found demonstrated that, surprisingly, both cell populations had both normal and the monobasic deletion mutant *CD20* genes. To determine the proportion of the genes, the PCR-amplified DNA fragments were inserted into a TA-cloning vector and 16 clones from both 'R-high' and 'R-low' fractions were determined the sequence of *CD20*. As a result, the ratio of mutant DNA accounted for approximately half of genomic DNA of both 'R-high' (7 out of 16) and 'R-low' (9 out of 16). On the other hand, the results of sequence analysis about the cDNA revealed that the ratio of mutant mRNA in 'R-low' was remarkably increased (14 out of 16), whereas that of 'R-high' was as the same of the results of genomic DNA (8 out of 16; Figure 4b). We also carried out a sequence analysis about genomic DNA from a slice of paraffin -embedded tissue of lymph node at the first diagnosis of this patient, and found that approximately half of the genomic DNA

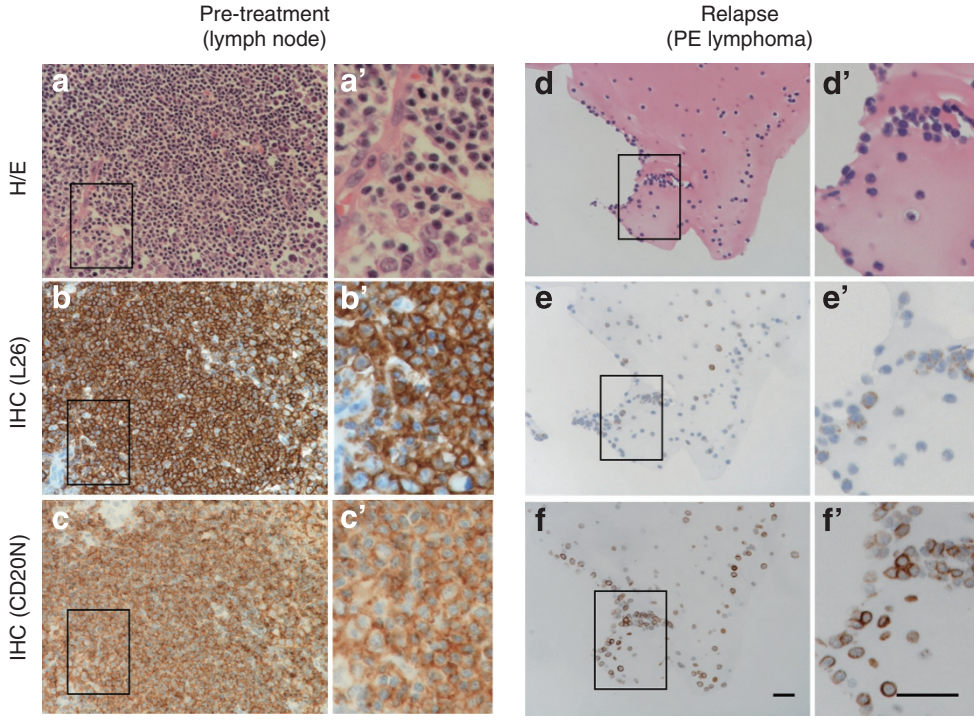

Figure 2 Immunohistochemistry (IHC) was performed on a biopsied specimen of a lymph node at the first examination (**a**, **b** and **c**) and on a fibrin clot from the B-cell population from pleural effusion at the relapse phase (**d**, **e** and **f**). Both L26 and CD20N antibodies uniformly stained the lymphoma cells in the lymph node biopsy specimen (**b** and **c**, respectively). However, L26 did not recognize about half of the B cells derived from pleural effusion (**e**), whereas CD20N stained almost all the cells (**f**). (**a** and **d**) indicates hematoxylin and eosin (H/E) stain. High-magnification images of the region boxed in (**a**–**f**) were shown in (**a**′–**f**′), respectively. An objective lens of × 60 was used, bar: 50 μm. PE lymphoma, lymphoma cell in pleural effusion.

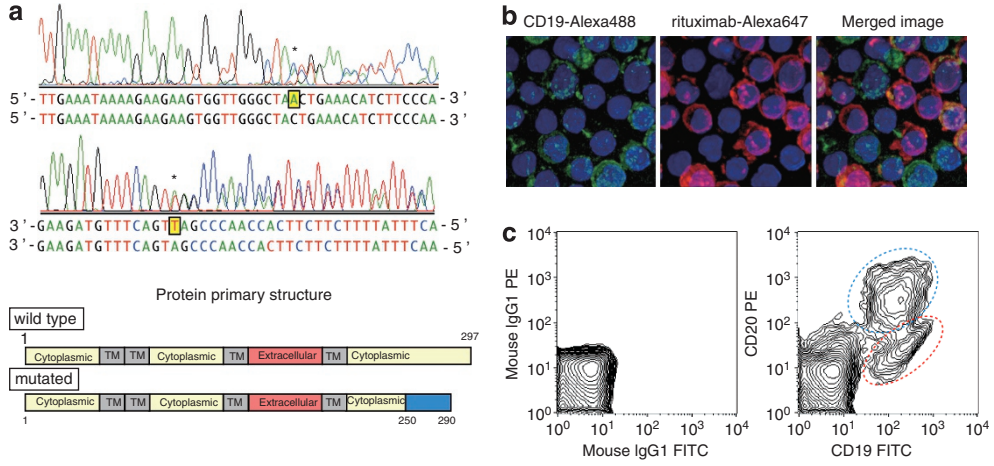

Figure 3 The analysis of primary lymphoma cells derived from pleural effusion of a patient with rituximab-refractory, diffuse large-cell lymphoma. (**a**) A direct sequence analysis of the CD20-coding region revealed that an adenine residue (+478) was deleted in about half of the cDNA. This gene mutation caused a frame shift after the amino-acid sequence of 250 and early denomination. The blue column in the protein schematic charts expresses an abnormal primary structure. *Single nucleotide deletion occurred at this position in approximately half of cDNA. (**b**) Rituximab-binding analysis based on three-dimensional imaging. Magnetically sorted living B-lineage cells were labeled with CD19 (green pseudo-color) and rituximab (red pseudo-color). Although the intensity varied, the CD19 antigen was expressed in most of the cells. Meanwhile, rituximab bound markedly to approximately half of the cells, but the binding to the rest of cells could not be detected. The blue pseudo-color indicates fluorescence of Hoechist22242 nuclear dye. Results shown here are representative of the 19 microscopic fields. (**c**) Flow cytometric analysis of mononuclear cells from the pleural effusion of this patient suggested that there were two populations of different CD20-expressing levels among CD19 positive cells. The mean fluorescence intensities (MFIs) of the higher (blue) and lower (red) CD20-expressing populations were calculated as 486.8 and 30.5, respectively. FITC, fluorescein isothiocyanate.

included the mutant *CD20* gene same as the cells at relapse (8 out of 16; Figure 4c). These results indicated that this patient had already carried the mutation in *CD20* gene, as onset of primary lymphoma, and that a transcriptional imbalance of wild-type *CD20* and mutated *CD20* have occurred by undetermined mechanisms in some cell populations.

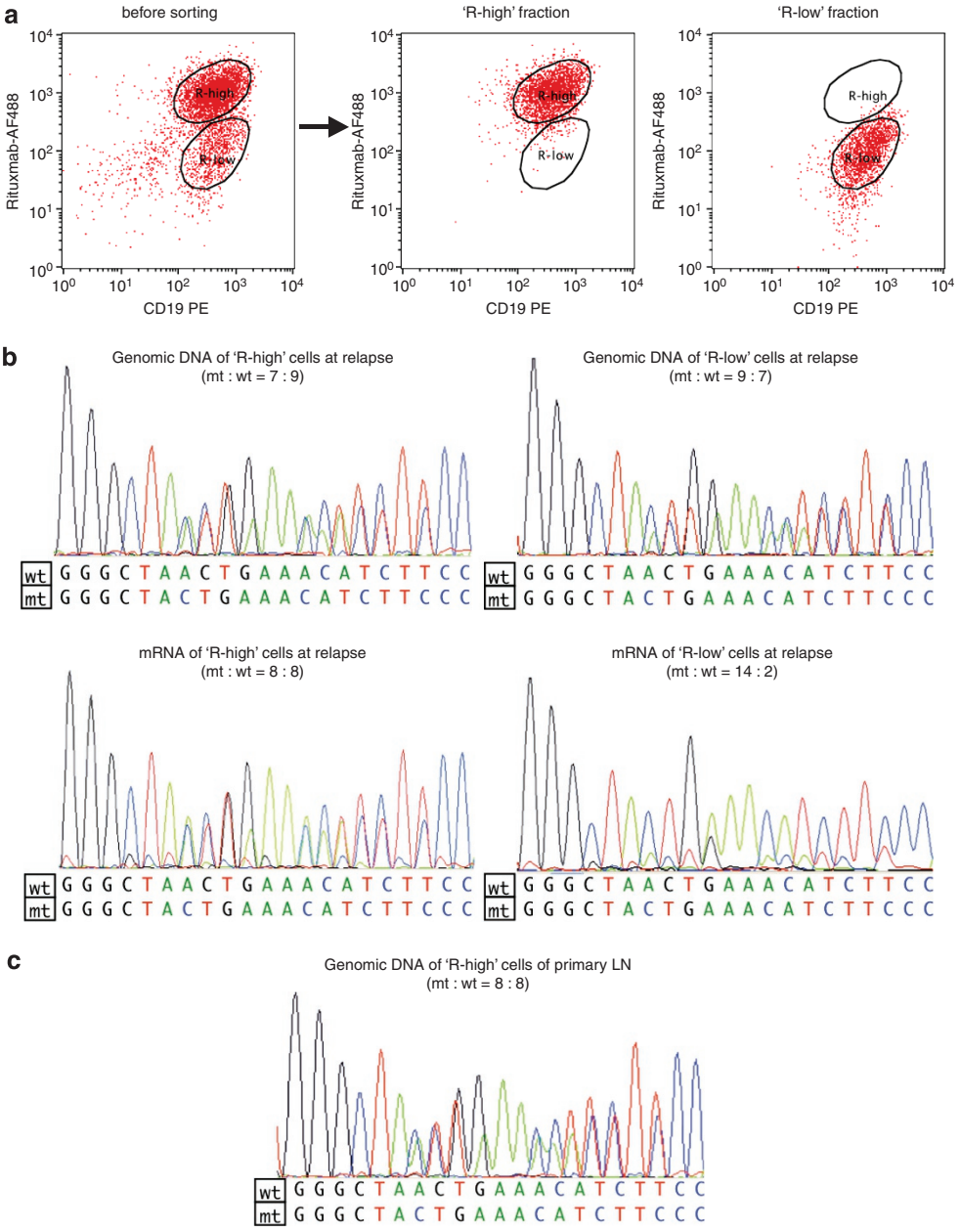

Figure 4 The genetic analysis of patient's lymphoma cells. The cryopreserved B linage cells of the pleural effusion at relapse were further sorted into two fractions of cells with high affinity to rituximab (R-high) and those of low (R-low) by using flow cytometry. (**a**) Dot blot of the cells before and after sorting. (**b**) The results of CD20 sequence analysis of genomic DNA and cDNA of 'R-high' and 'R-low'. The diagrams of direct sequencing of CD20 exon 8 region are shown. The ratio of mutant and wild-type *CD20* genes were determined by the sequencing of 16 clones of RT-PCR products. (**c**) The results of genomic DNA sequence of primary lymphoma.

As CD20 is thought to be present as a tetramer in cells,[7] mutated CD20 may affect also wild-type peptide in the same cell. To verify this possibility, we introduced the *CD20* gene carrying the same mutation as this patient to $CD20^-$ cell line, KMS12PE and $CD20^+$ Daudi using a retrovirus vector, then selected the cells expressing the exogeneous *CD20* by a green fluorescent protein reporter promoted by an internal ribosome entry site (Figure 5a). As the result of evaluating the binding affinity to rituximab by flow cytometry, the exogeneous mutated CD20 exhibited remarkably attenuated antigenicity to rituximab as compared with the wild-type CD20 (Figure 5b). Next, we transformed Daudi cells with the mutant *CD20* to examine the effect on expression of wild-type CD20 molecules. In consideration of turnover of intrinsic CD20, we evaluated binding of rituximab to the transfectants 7 days after virus infection. As shown in Figure 5c, the expression of this mutated CD20 was found to have hardly affected the affinity for rituximab. These results suggested that at least the mutation found in this patient did not exert a dominant negative effect against normal CD20 molecules.

Discussion

Previously, we reported that mutations in the *CD20* gene were found with some frequency in patients treated with rituximab.

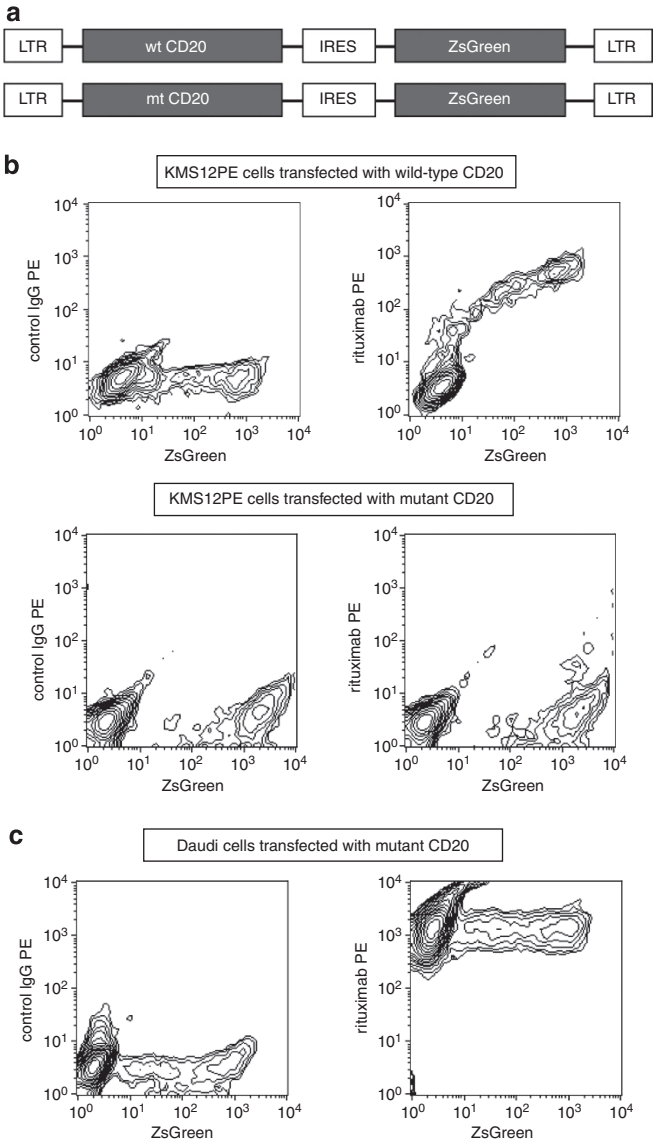

Figure 5 The effect of mutant *CD20* on wild-type *CD20* with respect to rituximab binding. (**a**) The schematic diagram of retrovirus vectors used for transduction of wild-type and mutant *CD20*. (**b**) The transfectants were labeled with PE-conjugated. rituximab and analyzed by flow cytometry at seven days after viral infection. The contour plots of KMS12PE cells transfected with wild-type (upper panel) or mutated *CD20* (lower panel) are shown. (**c**) Daudi cells were transfected with mutated *CD20* and analyzed the rituximab-binding. The mutant *CD20* introduced exogenously hardly affected the binding of rituximab to Daudi cells. IRES, internal ribosome entry site; LTR, long terminal repeat; wt, wild type; mt, mutant.

These cases often have a diagnosis of CD20 negative by immunostaining, based on the commonly used L26 antibody, and are difficult to distinguish from the cases in which protein expression of CD20 is extremely low. So the mutation in the *CD20* gene has been less noticed with regard to resistance to rituximab. In the present study, we roughly identified the epitope of L26, and it became clear that all of the C-terminal-mutated CD20 that we had found earlier lost the epitope for L26, because the epitope was located near the C-terminal of CD20 molecule. To detect CD20 with these mutations comprehensively, we developed monoclonal antibodies that recognize a part of the amino-acid sequence of the N-terminal cytoplasmic region of CD20. One of these antibodies, CD20N, recognized CD20 proteins, including those having a mutation in the paraffin-embedded, formalin-fixed specimen. In this study, we showed that it could be applied to the primary screening of the lymphoma cells that express mutated CD20 by selecting L26-negative and CD20N-positive cells.

To date, there are not many reports that the mutation of the *CD20* gene contributes to resistance to rituximab.[1,8] A part of the reason for this may be that L26 cannot detect most of mutated CD20. In addition, Johnson *et al*.[8] carried out a sequencing screening of exon 5 of the *CD20* gene encompassing the epitope of rituximab. They detected *CD20* mutations involving the rituximab epitope in only 1/264 (0.4%) and 1/15 (6%) of the biopsies taken at diagnosis and relapse, respectively. Similarly, in our previous screening, no mutation was found in the region of exon 5, whereas four cases with mutation (out of 50) were found in the C-terminal cytoplasm region of CD20.[1] In the *CD20* gene, a genetic mutation could be more likely to occur in the C-terminal region compared with around the region of rituximab epitope by uncertain mechanism(s).

By using live cryopreserved cells, derived from a newly identified case with the mutation in the *CD20* gene, we successfully analyzed in detail the phenotype of lymphoma cells having mutated CD20. In this case, a frame shift mutation occurred because of one base nucleotide deletion, resulting in the translation of peptide of another reading frame of 41 amino acids after the amino acid position 250 with a slight early termination. Immunohistochemical analysis using CD20N antibody revealed that the CD20 molecules with C-terminal mutations were indeed expressed in the lymphoma cells, and located at the cell membrane. However, the living cell binding evaluation showed that rituximab could scarcely bind to these cells. These results suggest that the C-terminal region of CD20 undertakes a critical role in presentation of the large loop in which the rituximab-binding site locates.

As a result of genetic analysis for lymphoma cells, it was suggested that this patient had a mutation in the *CD20* gene as onset of primary lymphoma. Because normal and mutated *CD20* gene were almost the same copy numbers and the most of cells in the lymph follicle were stained in L26 at the first diagnosis, it can be considered that the lymphoma cells of this patient had equal number of normal and mutated *CD20* alleles rather than the mixture of the cells having only normal *CD20* allele(s) or only mutant allele(s). And at the relapse, two cell populations of the different affinity for rituximab has arose ('R-high' and 'R-low'), and both had a genome of the same mutation status, however, the expression of the mutated mRNA has been predominant only in 'R-low'. As a result of semi-quantitative RT-PCR analysis revealed that whole *CD20* mRNA expression of 'R-low' slightly decreased as compared with that of 'R-high' (data not shown), the imbalanced mRNA expression in 'R-low' may be due to the suppression of *CD20* mRNA expression from the wild-type allele at the transcription level.

To summarize these data, the primary lymphoma cells of this patient expressed both wild-type and mutated *CD20* equally. As the mutant CD20 in this case was found to have little effect on the antigenicity of wild-type CD20 molecules, these cells were still susceptible to rituximab plus CHOP and the patient has obtained complete remission. However, at the relapse, cells that predominantly expressed the mutant CD20 emerged. This mutant molecule expressed and localized at the plasma membrane, however, the large loop could not be oriented appropriately. So it was considered that rituximab-containing salvage treatments have failed perhaps because affinity for rituximab was not enough.

It was noteworthy that the antibody that recognizes N-terminal region of CD20 has capability to detect the mutated CD20 before start of the salvage therapy. This indicated the possibility that we can predict the existence of lymphoma cells resistant to rituximab before start of therapy. In addition, this information may provide important criterion to judge whether it should switch to the treatment such as using second-generation CD20 antibody that is effective against fewer CD20-expressing cells[9–12] or using antibody for the different target molecule such as CD22.[13,14]

The resistance for a molecular target drug acquired by a mutation in the gene of the target molecule is commonly considered to be irreversible.[15–19] We propose here that detecting a mutation in the gene by screening using antibodies of two kinds of epitope is useful in detection of irreversible resistant mutation for molecular targeted drug including rituximab.

Conflict of interest

The authors declare no conflict of interest.

Acknowledgements

We thank Ms Sayuri Minowa, Ms Harumi Shibata and Ms Mariko Mikuniya for their assistance in specimen preparation. We also thank Dr Dovie Wylie of On-Site English, Inc. (Palo Alto, CA, USA) for English editing assistance.

References

1 Terui Y, Mishima Y, Sugimura N, Kojima K, Sakurai T, Kuniyoshi R *et al.* Identification of CD20 C-terminal deletion mutations associated with loss of CD20 expression in non-Hodgkin's lymphoma. *Clin Cancer Res* 2009; **15**: 2523–2530.
2 Mason DY, Comans-Bitter WM, Cordell JL, Verhoeven MA, van Dongen JJ. Antibody L26 recognizes an intracellular epitope on the B-cell-associated CD20 antigen. *Am J Pathol* 1990; **136**: 1215–1222.
3 Norton AJ, Isaacson PG. Monoclonal antibody L26: an antibody that is reactive with normal and neoplastic B lymphocytes in routinely fixed and paraffin wax embedded tissues. *J Clin Pathol* 1987; **40**: 1405–1412.
4 Hata H, Matsuzaki H, Matsuno F, Sonoki T, Takemoto S, Kuribayashi N *et al.* Establishment of a monoclonal antibody to plasma cells: a comparison with CD38 and PCA-1. *Clin Exp Immunol* 1994; **96**: 370–375.
5 Kohler G, Milstein C. Continuous cultures of fused cells secreting antibody of predefined specificity. *Nature* 1975; **256**: 495–497.
6 Mishima Y, Sugimura N, Matsumoto-Mishima Y, Terui Y, Takeuchi K, Asai S *et al.* An imaging-based rapid evaluation method for complement-dependent cytotoxicity discriminated clinical response to rituximab-containing chemotherapy. *Clin Cancer Res* 2009; **15**: 3624–3632.
7 Polyak MJ, Li H, Shariat N, Deans JP. CD20 homo-oligomers physically associate with the B cell antigen receptor. Dissociation upon receptor engagement and recruitment of phosphoproteins and calmodulin-binding proteins. *J Biol Chem* 2008; **283**: 18545–18552.
8 Johnson NA, Leach S, Woolcock B, deLeeuw RJ, Bashashati A, Sehn LH *et al.* CD20 mutations involving the rituximab epitope are rare in diffuse large B-cell lymphomas and are not a significant cause of R-CHOP failure. *Haematologica* 2009; **94**: 423–427.
9 Pawluczkowycz AW, Beurskens FJ, Beum PV, Lindorfer MA, van de Winkel JG, Parren PW *et al.* Binding of submaximal C1q promotes complement-dependent cytotoxicity (CDC) of B cells opsonized with anti-CD20 mAbs ofatumumab (OFA) or rituximab (RTX): considerably higher levels of CDC are induced by OFA than by RTX. *J Immunol* 2009; **183**: 749–758.
10 Hagenbeek A, Gadeberg O, Johnson P, Pedersen LM, Walewski J, Hellmann A *et al.* First clinical use of ofatumumab, a novel fully human anti-CD20 monoclonal antibody in relapsed or refractory follicular lymphoma: results of a phase 1/2 trial. *Blood* 2008; **111**: 5486–5495.
11 Patz M, Isaeva P, Forcob N, Muller B, Frenzel LP, Wendtner CM *et al.* Comparison of the *in vitro* effects of the anti-CD20 antibodies rituximab and GA101 on chronic lymphocytic leukaemia cells. *Br J Haematol* 2011; **152**: 295–306.
12 Mossner E, Brunker P, Moser S, Puntener U, Schmidt C, Herter S *et al.* Increasing the efficacy of CD20 antibody therapy through the engineering of a new type II anti-CD20 antibody with enhanced direct and immune effector cell-mediated B-cell cytotoxicity. *Blood* 2010; **115**: 4393–4402.
13 Dijoseph JF, Dougher MM, Armellino DC, Evans DY, Damle NK. Therapeutic potential of CD22-specific antibody-targeted chemotherapy using inotuzumab ozogamicin (CMC-544) for the treatment of acute lymphoblastic leukemia. *Leukemia* 2007; **21**: 2240–2245.
14 DiJoseph JF, Goad ME, Dougher MM, Boghaert ER, Kunz A, Hamann PR *et al.* Potent and specific antitumor efficacy of CMC-544, a CD22-targeted immunoconjugate of calicheamicin, against systemically disseminated B-cell lymphoma. *Clin Cancer Res* 2004; **10**: 8620–8629.
15 Pao W, Miller VA, Politi KA, Riely GJ, Somwar R, Zakowski MF *et al.* Acquired resistance of lung adenocarcinomas to gefitinib or

erlotinib is associated with a second mutation in the EGFR kinase domain. *PLoS Med* 2005; **2**: e73.
16 Engelman JA, Janne PA. Mechanisms of acquired resistance to epidermal growth factor receptor tyrosine kinase inhibitors in non-small cell lung cancer. *Clin Cancer Res* 2008; **14**: 2895–2899.
17 Shah NP, Sawyers CL. Mechanisms of resistance to STI571 in Philadelphia chromosome-associated leukemias. *Oncogene* 2003; **22**: 7389–7395.
18 Shah NP, Nicoll JM, Nagar B, Gorre ME, Paquette RL, Kuriyan J *et al.* Multiple BCR-ABL kinase domain mutations confer polyclonal resistance to the tyrosine kinase inhibitor imatinib (STI571) in chronic phase and blast crisis chronic myeloid leukemia. *Cancer Cell* 2002; **2**: 117–125.
19 Wang SE, Narasanna A, Perez-Torres M, Xiang B, Wu FY, Yang S *et al.* HER2 kinase domain mutation results in constitutive phosphorylation and activation of HER2 and EGFR and resistance to EGFR tyrosine kinase inhibitors. *Cancer Cell* 2006; **10**: 25–38.